Sub-nanosecond Optical Switching Using Chip-Based Soliton Microcombs

S. Lange[1]*, A. S. Raja[2], K. Shi[1], M. Karpov[2], R. Behrendt[1], D. Cletheroe[1], I. Haller[1], F. Karinou[1], X. Fu[2], J. Liu[2], A. Lukashchuk[2], B. Thomsen[1], K. Jozwik[1], P. Costa[1], T. J. Kippenberg[2], H. Ballani[1]

[1]*Microsoft Research, 21 Station Road, Cambridge, CB1 2FB, U.K.*

[2]*Swiss Federal Institute of Technology Lausanne (EPFL), Lab of Photonics& Quantum Measurements, 1015 Lausanne, Switzerland.*

**t-solang@microsoft.com*

Abstract: We demonstrate sub-nanosecond wavelength switching, using a chip-based soliton microcomb and a semiconductor optical amplifier-based wavelength selector. 50-Gbps PAM4 transmission is achieved with discrete components and 25-Gbps NRZ with a photonic integrated wavelength selector.

OCIS codes: 060.4510, 130.4815, 190.4390, 250.5300, 250.5980

1. Introduction

Today's data centre (DC) networks comprise a hierarchy of electrical switches, interconnected using optical fibres, which require power-hungry opto-electrical transceivers at each hop. Optical circuit switching (OCS) constitutes a promising alternative to decrease the power consumption (by reducing the number of electrical switches and transceivers) and to lower network latency (by eliminating network buffers) [1]. In particular, wavelength switching based on tunable lasers and arrayed waveguide grating routers (AWGRs) [2] has received much attention recently due to its potential to achieve nanosecond-scale switching, required to efficiently handle small-packet DC workloads [3], as well as to improve the overall network resilience and simplify deployment by eliminating active elements in the network core. Wavelength-switching performance is directly tied to the laser's tuning time, which is mainly limited by the electrical carrier dynamics in the tuning sections, resulting in tuning times ranging from 80 ns for optimised off-the-shelf tuneable lasers [4] to 5 ns for custom designs [5]. Shi et al. [3] demonstrated sub-nanosecond wavelength switching time (3.84 ns end-to-end switching latency) by disaggregating the light generation from the wavelength selection functionality of the tuneable laser [6]. Their demonstration used a bank of discrete laser sources for light generation and an array of semiconductor optical amplifiers (SOAs) for the wavelength selection.

In this paper, we propose a disaggregated tunable laser (Fig. 1(a)), comprising of a chip-based soliton microcomb [7], as the multi-wavelength source, and a wavelength selector to achieve fast wavelength switching independent of the tuning range. Chip-based soliton microcombs have been demonstrated as an efficient source for multi-wavelength lasers. Their broad-bandwidth operation across C- and L-bands, precise dispersion engineering (50/ 100 GHz spacing), wafer-scale scalability and the potential for lower power consumption in the future make this system attractive for wavelength switching with several tens of wavelengths in comparison to using a bank of lasers [8]. More importantly, no complex electronics or extra guard band are required to align the individual lasing wavelengths accurately to the wavelength selector thanks to the equal frequency spacing of the comb lines [8]. Co-packaged optics [9] makes it easy to share the light source across a bank of modulators within the same package. This is particularly attractive for the proposed comb-based tuneable source as its cost and power can be amortized across many transceivers while still retaining the benefits described above. We present a proof-of-concept, including a Si_3N_4 soliton microcomb and an array of discrete SOAs as wavelength selector. SOAs are chosen as ON/OFF gates due to their fast switching speed, small form factor and high extinction ratio. We demonstrate less than 520 ps wavelength switching time, 25 GBd non-return-to-zero on-off keying (NRZ) and four-level pulse amplitude modulation (PAM4) burst-mode transmission. We also show similar performance when using our indium phosphide (InP)-based wavelength-selector photonic integrated circuit (PIC) with 25 GBd NRZ transmission.

2. Soliton microcomb description

A photonic chip-based soliton microcomb generates equally spaced coherent signals. One important platform to generate soliton microcombs is Si_3N_4 due to ultra-low losses, absence of two-photon absorption at 1550 nm (bandgap~ 5 eV) and CMOS-compatibility. Chip-scale laser pumped solitons have been demonstrated, enabling fully integrated comb systems [10]. The Si_3N_4 micro-resonator is fabricated using the photonic damascene process with a reflow step, which enables mean intrinsic Q-factors of more than 15 million [11]. The fabricated device has a free spectral range of 99.5 GHz, which is sufficiently close to the ITU grid. The micro-resonator is packaged with an ultra-high numerical aperture fibre (UHNA), which is spliced with standard single-mode fibre, resulting in 15% fibre-chip-fibre coupling efficiency.

The comb source is shown in Fig. 1(a). A continuous wave (CW) 1550 nm fibre laser is used in conjunction with an

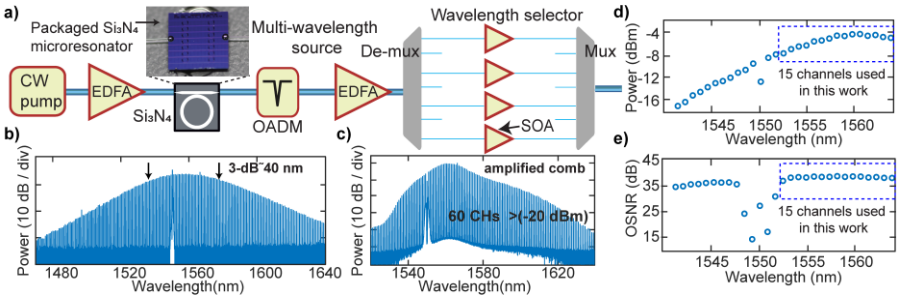

Fig. 1. a) Tuneable laser source based on a soliton microcomb and an SOA-based wavelength selector; b) Soliton microcomb optical output spectrum, c) Optical spectrum after EDFA, d) Output power/ch. after EDFA, e) OSNR/ch. after EDFA.

erbium-doped fibre amplifier (EDFA) to pump the micro-resonator. At 1.2 W input power, a multi-soliton state is initiated by performing a scan over the resonance, then a single soliton (Fig. 1(b)) is generated via backward switching. The comb channels are aligned to the ITU grid using a thermoelectric cooler (TEC). After filtering the pump, using an optical add and drop multiplexer (OADM), the soliton is amplified with a low-noise EDFA, giving 60 channels in the C- and L-band with an output power larger than -20 dBm (Fig. 1(c)). In the C-band, the power per channel is up to -4 dBm (Fig. 1(d)). The optical signal-to-noise ratio (OSNR) per channel (Fig. 1(e)) around the pump laser wavelength is degraded due to the pump EDFA amplified spontaneous emission noise. In this work, we use 15 comb channels between 1552.5 nm to 1563.9 nm with an output power of > -20 dBm and an OSNR> 34 dB.

3. 25 GBd burst-mode NRZ and PAM4 operation

The experimental setup is shown in Fig. 2(a). The comb source output is de-multiplexed using a 1×48 channel, 100 GHz-spaced arrayed waveguide grating (AWG) with more than 30 dB isolation between the channels. Four of the AWG outputs are input to SOAs (small-signal gain: 11-13 dB at 1550 nm), which reside on a custom-designed electronic circuit board that provides the bias currents and generates the ON/OFF switching signals. A timing board provides an external reference clock. The SOA outputs are combined and amplified by an EDFA. An 18-nm optical bandpass filter (OBF) is used to suppress unneeded comb channels and out-of-band noise from the SOAs and the EDFA. The burst-mode data sequences are generated using a 25 GHz DAC. A Mach-Zehnder modulator (MZM) applies a 25 GBd burst-mode NRZ or PAM4 random sequence with 2^{15}- and 2^{16}-bits length, respectively. Each burst consists of a header sequence that contains 32 symbols (1.28 ns) and a payload sequence that contains 1024 symbols (40.96 ns) at 25 GBd. There is a 2.56 ns guard zone between adjacent bursts. The 50 GHz photodetector (PD) output is amplified by a 20 GHz electrical amplifier and the signal is captured on a 160 GSamples/s real-time scope and processed offline to obtain the bit error rate (BER) performance. Firstly, we characterize the switching performance for 15 channels. The 10 %× 90 % rise and fall times for each channel are shown in Fig. 2(b) with a maximum rise and fall time of 520 ps and 405 ps, respectively . We then characterise the transmitter BER vs received optical power (ROP) under fast wavelength switching operation, while switching between two comb channels with different spacings: 11.3 nm (CH34-48), 5.7 nm (CH37-44) and 0.8 nm (CH39-40). When switching between multiple channels, the signals (Fig. 2(c)) are aligned to the reference clock and adjusted to a constant power by tuning the SOA bias currents. At 25 GBd PAM4, BER performance below the 5×10^{-5} FEC threshold is achieved for all three combinations for an ROP of around -7 dBm to -8 dBm (Fig. 2(d)). BER error floors are arising for input power higher than -6 dBm due to the accumulated amplifier noise and the AWG crosstalk. Then we measure the BER when switching between four channels sequentially. Transmission below the FEC threshold is achieved at 25 GBd NRZ

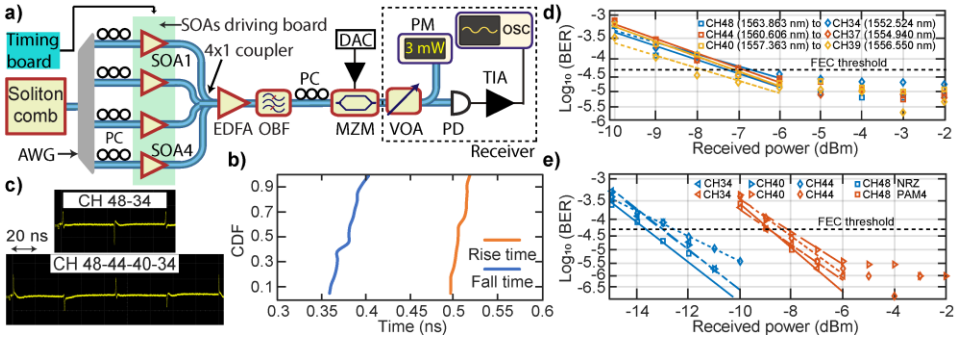

Fig. 2. a) Experimental setup for burst-mode NRZ/ PAM4 transmission b) Rise and fall times cumulative distribution function (CDF), c) 2 ch. and 4 ch. switching signals; 25 GBd burst-mode BER vs received power: d) 2 ch PAM4, e) 4 ch NRZ and PAM4.

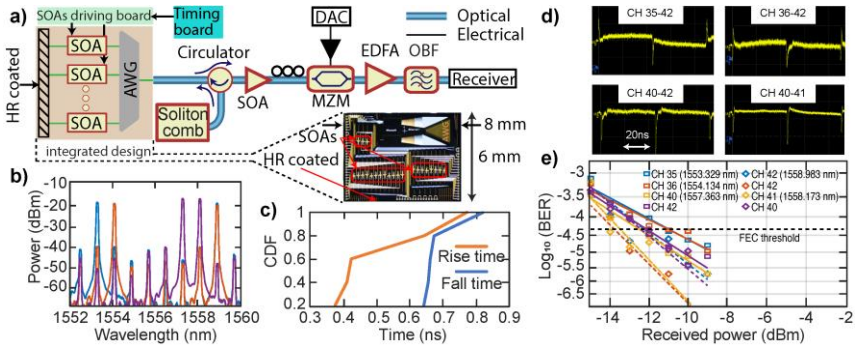

Fig 3. a) Experimental setup with wavelength selector PIC; Tuneable laser b) Optical spectra, c) Rise and fall times CDF, d) 2 ch. switching signals, e) 25 GBd NRZ BER vs. ROP.

and PAM4 for a ROP larger than -12.3 dBm and -8 dBm, respectively (Fig. 2(e)).

4. 25 GBd burst-mode NRZ operation using a custom designed wavelength selector PIC

The experimental setup with the wavelength selector PIC described in [3] is given in Fig 3(a). A 32 channel AWG with 50 GHz channel spacing is used simultaneously as the MUX/DEMUX, which is enabled by a high-reflection (HR) coating on one of the PIC facets. SOAs are integrated to nineteen of the AWG outputs. Two SOAs are contacted with RF probes, while a TEC is used to stabilise the PIC temperature. The PIC output is coupled to an anti-reflection coated tapered fibre and the SOA bias currents and ON/OFF switching signals are provided by the SOA driving board. The comb laser is launched into the PIC through an optical circulator. Since the PIC output power is below the EDFA input power limit, a SOA is used for amplification. An additional EDFA is inserted after the MZM for increasing the ROP. By adjusting the PIC temperature, seven of the comb channels can be aligned to the AWG. Two-channel 25 GBd NRZ operation is tested at four different channel spacings: 5.7 nm (CH35-42), 4.8 nm (CH36-42), 1.6 nm (CH40-42) and 0.8 nm (CH40-41). The optical spectra after the tuneable laser source (Fig 3(b)) have a channel isolation larger than 21 dB. The received channel powers are aligned by adjusting the MZM input polarisation. The measured 10 %- 90 % switching times (Fig 3(c)) increase at lower comb channel power and are between 640 ps to 820 ps for the five channels. By optimising the SOA bias currents, the 2-channel switching signals (Fig 3(d)) are adjusted to minimise overshoots, while maintaining a fast rising edge. For 25 GBd PAM4 operation, the signal-to-noise ratio must be further improved, i.e. by increasing the microcomb output power to reduce amplifier noise, by increasing the AWG channel isolation and by reducing the passive insertion loss on the PIC. The 25 GBd NRZ BER vs. ROP results are depicted in Fig 3(e). BER performance below the FEC threshold is achieved for all combinations at an ROP larger than -11 dBm. The variations stem from the different power and shapes of the switching signals. The results show the feasibility of the integrated tuneable laser source for 25 GBd NRZ transmission.

5. Conclusions and future work

We showed the feasibility of achieving sub-ns wavelength switching using a soliton microcomb multi-wavelength laser source, followed by an SOA-based wavelength selector to enable OCS in future DC networks. 25 GBd NRZ and PAM4 transmission below the 5×10^{-5} FEC limit is achieved, using off-the-shelf SOAs. Our results have been further validated employing a custom designed PIC with NRZ signalling. Further optimisation of the tuneable laser is ongoing to increase the output power and power efficiency, e.g. by improving the coupling efficiency of the packaged Si_3N_4 chip and by employing an EDFA after the microcomb with a flat and maximum gain in the C-band. Research is also ongoing to reduce the microcomb frequency spacing to 50 GHz to match the one of the wavelength selector PIC.

6. References

[1] H. Ballani *et al.*, OFC 2018.
[2] R. Proietti *et al.*, in *Optical Switching in Next Generation Data Centers*, Springer, 2018.
[3] K. Shi *et al.*, ECOC 2019.
[4] A. C. Funnell *et al.*, *J. Light. Technol.*, vol. 35, no. 20, Oct. 2017.
[5] J. E. Simsarian *et al.*, *IEEE Photonics Technol. Lett.*, vol. 18, no. 4, Feb. 2006.
[6] G. de Valicourt *et al.*, ECOC 2014.
[7] V. Brasch *et al.*, *Science*, vol. 351, no. 6271, Jan. 2016.
[8] P. Marin-Palomo *et al.*, *Nature*, vol. 546, no. 7657, 2017.
[9] A. V. Krishnamoorthy *et al.*, in *2016 IEEE Optical Interconnects Conference (OI)*, 2016.
[10] A. S. Raja *et al.*, *Nat. Commun.*, vol. 10, no. 1, Feb. 2019.
[11] M. H. P. Pfeiffer *et al.*, *Optica*, vol. 5, no. 7, Jul. 2018.